

# SPREAD SPECTRUM FOR COMPRESSED SENSING TECHNIQUES IN MAGNETIC RESONANCE IMAGING

Y. Wiaux<sup>1,2,3</sup>, G. Puy<sup>1,4</sup>, R. Gruetter<sup>4</sup>, J.-Ph. Thiran<sup>1</sup>, D. Van De Ville<sup>2,3</sup>, P. Vanderghenst<sup>1</sup>

<sup>1</sup>Institute of Electrical Engineering, Ecole Polytechnique Fédérale de Lausanne (EPFL), CH-1015 Lausanne, Switzerland

<sup>2</sup>Institute of Bioengineering, Ecole Polytechnique Fédérale de Lausanne (EPFL), CH-1015 Lausanne, Switzerland

<sup>3</sup>Department of Radiology and Medical Informatics, University of Geneva (UniGE), CH-1211 Geneva, Switzerland

<sup>4</sup>Institute of the Physics of Biological Systems, Ecole Polytechnique Fédérale de Lausanne (EPFL), CH-1015 Lausanne, Switzerland

## ABSTRACT

Magnetic resonance imaging (MRI) probes signals through Fourier measurements. Accelerating the acquisition process is of major interest for various MRI applications. The recent theory of compressed sensing shows that sparse or compressible signals may be reconstructed from a small number of random measurements in a sensing basis incoherent with the sparsity basis. In this context, we advocate the use of a chirp modulation of MRI signals prior to probing an incomplete Fourier coverage, in the perspective of accelerating the acquisition process relative to a standard setting with complete coverage. We analyze the spread spectrum phenomenon related to the modulation and we prove its effectiveness in enhancing the overall quality of image reconstruction. We also study its impact at each scale of decomposition in a wavelet sparsity basis. Our preliminary results rely both on theoretical considerations related to the mutual coherence between the sparsity and sensing bases, as well as on numerical simulations from synthetic signals.

**Index Terms**— magnetic resonance imaging, compressed sensing, spread spectrum

## 1. COMPRESSED SENSING

It is well-known that a large variety of natural signals are sparse or compressible in multi-scale decompositions, such as wavelet bases. A band-limited signal may be expressed as the  $N$ -dimensional vector of its values sampled at the Nyquist-Shannon rate. By definition, a signal is sparse or compressible in some basis if its expansion contains only a small number  $K \ll N$  of non-zero or significant components, respectively. The theory of compressed sensing demonstrates that a small number  $M \ll N$  of random measurements, in a sensing basis incoherent with the sparsity basis, will suffice for an accurate

and stable reconstruction of such signals [1]. The basic framework proposes to solve the Basis Pursuit (BP) minimization problem for the signal recovery. This problem regularizes the originally ill-posed inverse problem by an explicit sparsity prior. In the presence of noise, the so-called Basis Pursuit denoise (BP <sub>$\epsilon$</sub> ) problem is the minimization of the  $\ell_1$  norm of the components of the signal in the sparsity basis  $\Psi$  under a constraint on the  $\ell_2$  norm of the residual noise.

In particular, random Fourier measurements of a signal sparse in image space represent a good sensing procedure. The mutual coherence  $\mu(F, \Psi)$  between the Fourier basis  $F$  and the sparsity basis  $\Psi$  may be defined as the maximum complex modulus of the scalar product between vectors of the two bases. In other words, this mutual coherence identifies with the maximum complex modulus of the Fourier coefficients of the sparsity basis vectors. It plays an essential role in the signal reconstruction quality as, according to the theory, for fixed  $M$ , the sparsity recovered increases with the mutual incoherence, i.e. the inverse of the coherence, as  $K \propto \mu^{-2}(F, \Psi)$ . The incoherence is maximum between the Fourier basis and the image space basis identified by a sparsity matrix  $\Psi \equiv \Delta$  made up of unit spikes:  $\mu(F, \Delta) = N^{-1/2}$ .

## 2. MAGNETIC RESONANCE IMAGING

In the standard setting, considering two-dimensional imaging, MRI data provide a noisy and complete coverage of the Fourier plane, commonly named  $k$ -space, of the original image  $\rho$  of interest. In ideal conditions, this signal is a real and positive scalar function  $\rho(l)$  of the position  $l \in \mathbb{R}^2$ , with components  $(l, m)$ , representing the intensity of the magnetization induced by resonance in the tissues to be imaged.

In the present work, we consider the important issue of accelerating the MRI acquisition process, by reducing the number of  $k$ -space measurements, hence identifying an incomplete Fourier coverage, while maintaining the required reconstruction quality. This problem is equivalent to the question of enhancing the image reconstruction quality achievable at

This work is supported in part by the Center for Biomedical Imaging (CIBM) of the Geneva and Lausanne Universities, EPFL, and the Leenaards and Louis-Jeantet foundations, in part by the Swiss National Science Foundation (SNSF) under grant PP00P2-123438, and also by Merck Serono S.A..

a fixed number  $M \ll N$  of measurements. The issue of reconstructing the original  $N$ -dimensional vector identifying the image from these data is an ill-posed inverse problem.

We address the problem in a compressed sensing perspective. The signal exhibits some sparsity  $K \ll N$  in a chosen sparsity basis  $\Psi$ , and the sensing basis is identified by the Fourier basis  $F$ . In this context, the larger the typical size, in image space, of the waveforms constituting the sparsity basis, the smaller their extension in  $\mathbf{k}$ -space. As a consequence, the incoherence between the sparsity and sensing bases is decreased, which leads to a degradation of the reconstruction quality for given  $K$  and  $M$ .

The great flexibility in MRI scanners to tune magnetic field gradients and tailor radio frequency (RF) pulses might actually provide a response to this issue. Specifically, the use of quadratic phase profiles was advocated for various purposes, such as reduction of aliasing artifacts [2, 3] or improvement of dynamic range [4, 5]. This technique is known as phase scrambling and consists in altering the original image by a modulation such as a linear chirp  $C^{(w)}(|\mathbf{l}|) = e^{i\pi w|\mathbf{l}|^2}$ , where the norm  $|\mathbf{l}|$  corresponds to the distance to the center of the field-of-view, with the chirp rate  $w$  controlled by the intensity of the quadratic profile. This type of modulation can be obtained by using dedicated coils or by changing the RF pulse.

From the mathematical point of view, each corresponding measurement at spatial frequency  $\mathbf{k}$  identifies with the Fourier transform of the modulated planar signal:  $\nu(\mathbf{k}) = \widehat{C^{(w)}\rho(\mathbf{k})}$ . In  $\mathbf{k}$ -space, the modulation amounts to the convolution of the Fourier transform of the modulation with that of the signal:  $\widehat{C^{(w)}\rho} = \widehat{C^{(w)}} \star \widehat{\rho}$ . This convolution inevitably spreads the two-dimensional sample power spectrum of the signal, i.e. the square modulus of its Fourier transform, while preserving its overall norm. This spread spectrum phenomenon increases the incoherence between the sparsity and sensing bases.

A linear chirp  $C^{(w)}(|\mathbf{l}|)$  with chirp rate  $w$  is characterized by an instantaneous frequency  $w\mathbf{l}$  at position  $\mathbf{l}$ . On a finite field-of-view it is approximately a band-limited function. In each basis direction, the band limit of the signal after convolution  $B^{(C^{(w)}\rho)}$  is the sum of the individual band limits of the original signal  $B^{(\rho)}$  and of the chirp modulation  $B^{(C^{(w)})}$ . This simple consideration quantifies the spread spectrum phenomenon associated with the chirp modulation. A large variety of modulations would be suitable for this purpose, provided that they have a large enough band limit in  $\mathbf{k}$ -space, so that the spread spectrum phenomenon is significant.

Let us acknowledge the fact that the interest of compressed sensing for MRI was already proven [6]. The introduction of a signal modulation was recently proposed and tested on real data [7], but no theoretical underpinning neither guarantees relative to the reconstruction quality was proposed. Very recently, the spread spectrum technique proposed here was extensively studied by three of the authors in

the context of radio interferometry [8, 9].

### 3. DICTIONARIES AND INVERSE PROBLEM

The band-limited functions considered are completely identified by their Nyquist-Shannon sampling on a discrete uniform grid of  $N = N^{1/2} \times N^{1/2}$  points  $\mathbf{l}_i \in \mathbb{R}^2$  in image space, with  $1 \leq i \leq N$ . The sampled signal is denoted by a vector  $\boldsymbol{\rho} \in \mathbb{R}^N \equiv \{\rho_i \equiv \rho(\mathbf{l}_i)\}_{1 \leq i \leq N}$ . The chirp is complex and reads as the vector  $\mathbf{C}^{(w)} \in \mathbb{C}^N \equiv \{C_i^{(w)} \equiv C^{(w)}(|\mathbf{l}_i|)\}_{1 \leq i \leq N}$ . Because of the finite field-of-view, the functions may equivalently be described by  $\mathbf{k}$ -space components on a discrete uniform grid of  $N = N^{1/2} \times N^{1/2}$  spatial frequencies  $\mathbf{k}_i$ , with  $1 \leq i \leq N$ . This grid is limited at some maximum frequency defining the band limit.

We assume that the spatial frequencies  $\mathbf{k}$  probed during acquisition belong to the discrete grid of points  $\mathbf{k}_i$ . The  $\mathbf{k}$ -space coverage provided by the  $M/2$  spatial frequencies probed  $\mathbf{k}_b$ , with  $1 \leq b \leq M/2$ , can simply be identified by a binary mask in  $\mathbf{k}$ -space equal to 1 for each spatial frequency probed and 0 otherwise. The components measured may be denoted by a vector of  $M/2$  complex  $\mathbf{k}$ -space components  $\boldsymbol{\nu} \in \mathbb{C}^{M/2} \equiv \{\nu_b \equiv \nu(\mathbf{k}_b)\}_{1 \leq b \leq M/2}$ , corresponding to  $M$  real measures, and inevitably affected by complex noise of instrumental origin, identified by the vector  $\mathbf{n} \in \mathbb{C}^{M/2} \equiv \{n_b \equiv n(\mathbf{k}_b)\}_{1 \leq b \leq M/2}$ . Relying on the flexibility of realistic measurement distributions, we also assume that the spatial frequencies  $\mathbf{k}_b$  probed arise from a uniform random selection of  $\mathbf{k}$ -space frequencies. This allows us to discard considerations related to specific acquisition sequences. It also allows us to place our discussion in a setting which complies directly with the requirement of the theory of compressed sensing for random measurements.

In this discrete setting, the assumed  $\mathbf{k}$ -space coverage is incomplete with a number of real constraints  $M$  smaller than the number of unknowns  $N$ :  $M \ll N$ . An ill-posed inverse problem is thus defined for the reconstruction of the signal  $\boldsymbol{\rho}$  from the measurements  $\boldsymbol{\nu}$ :

$$\boldsymbol{\nu} \equiv \Phi^{(w)} \boldsymbol{\rho} + \mathbf{n} \text{ with } \Phi^{(w)} \equiv \text{MFC}^{(w)}, \quad (1)$$

where the matrix  $\Phi^{(w)} \in \mathbb{C}^{(M/2) \times N}$  identifies the complete linear relation between the signal and the measurements. The matrix  $\mathbf{C}^{(w)} \in \mathbb{C}^{N \times N} \equiv \{C_{ij}^{(w)} \equiv C_i^{(w)} \delta_{ij}\}_{1 \leq i, j \leq N}$  is the diagonal matrix implementing the chirp modulation. The unitary matrix  $\mathbf{F} \in \mathbb{C}^{N \times N} \equiv \{F_{ij} \equiv e^{-2i\pi \mathbf{k}_i \cdot \mathbf{l}_j / N^{1/2}}\}_{1 \leq i, j \leq N}$  implements the discrete Fourier transform. The matrix  $\mathbf{M} \in \mathbb{R}^{(M/2) \times N} \equiv \{M_{bj}\}_{1 \leq b \leq M/2; 1 \leq j \leq N}$  is the rectangular binary matrix implementing the mask characterizing the incomplete Fourier coverage. It contains only one non-zero value on each line, at the index of the  $\mathbf{k}$ -space coefficient corresponding to each of the spatial frequencies probed  $\mathbf{k}_b$ .

Without loss of generality, we simply consider the sparsity of the signals under scrutiny in a Haar wavelet basis  $\Psi$  on

the grids used. The sparsity basis is identified by the Haar wavelets at four scales indexed by integer values  $s$  with  $s = 1$  to  $s = 4$ , completed by the corresponding lowpass scaling function, identified by  $s = 5$ . The larger the value of the wavelet scale  $s$  with  $1 \leq s \leq 5$ , the larger the extent of the waveform in image space.

#### 4. EXPERIMENTAL SET UP

The synthetic signal  $\rho$  that we consider is the well-known Shepp-Logan phantom in some arbitrary intensity units, sampled on a grid of  $N = 256 \times 256 = 65536$  pixels on some field-of-view  $L = L^{1/2} \times L^{1/2}$ . The signal is illustrated in Fig. 1. Notice that it exhibits by definition exactly sparse magnitude of the gradient. The image could therefore naturally be reconstructed by solving the well-known analysis-based Total Variation ( $\text{TV}_\epsilon$ ) problem, which consists in the minimization of the  $\ell_1$  norm of the magnitude of the gradient of the signal under a constraint on the  $\ell_2$  norm of the residual noise. This perspective was actually concisely considered as an illustration in [9]. The choice of a generic wavelet basis is certainly suboptimal as the signal is not exactly sparse in such a basis. But it is still compressible, given the strong localization of the signal variations in image space. This choice will allow us to analyze the quality of the  $\text{BP}_\epsilon$  reconstruction in each wavelet band separately. Moreover it is more realistic as often, either true signals are not exactly sparse in any basis, or the sparsity basis is not known exactly.

Observations are considered for various numbers  $M/2$  of complex measurements corresponding to coverages of 4, 6, 8, 10, 15, 20, and 40 per cent of the  $\mathbf{k}$ -space. A small amount of instrumental noise is also added as independent identically distributed Gaussian noise. The component  $w$  may also be written in terms of a discrete component  $w_d$  as  $w = w_d N^{1/2}/L$ . We consider the values  $w_d = 0$  and  $w_d = 1$ . The case  $w_d = 0$  identifies the absence of modulation. The case  $w_d = 1$  corresponds to a linear chirp modulation with a maximum instantaneous frequency, i.e. an approximate band limit, equal to the band limit accessible on the grids considered. The chirp is illustrated in Fig. 1.

A number of 30 simulations are generated for each value of  $w_d$  and  $M$  considered, with independent noise and mask realizations. The measurements are simulated and the signals are reconstructed through the  $\text{BP}_\epsilon$  problem, solved by convex optimization. The quality of reconstruction is analyzed in terms of the corresponding signal-to-noise ratio (SNR).

#### 5. SPREAD SPECTRUM AND COHERENCES

The sensing basis as seen from the sparsity basis itself reads as  $\Theta^{(w)} \equiv \Phi^{(w)}\Psi \equiv \text{MFC}^{(w)}\Psi$ . One can formally reorganise this decomposition into modified sensing and sparsity bases, respectively  $\tilde{\Phi} \equiv \text{MF}$  and  $\tilde{\Psi}^{(w)} \equiv \text{C}^{(w)}\Psi$ . In this perspective, the mutual coherence  $\mu(\text{FC}^{(w)}, \Psi)$  identifies

	$s = 5$	$s = 3$	$s = 1$
$w_d = 0$	<b><math>6.250 \cdot 10^{-2}</math></b>	$2.272 \cdot 10^{-2}$	$6.014 \cdot 10^{-3}$
$w_d = 1$	<b><math>5.912 \cdot 10^{-2}</math></b>	$2.265 \cdot 10^{-2}$	$6.014 \cdot 10^{-3}$

**Table 1.** Values with four significant figures of the mutual coherences  $\mu(\text{FC}^{(w)}, \Psi^{(s)})$  between the sparsity and sensing bases, for the wavelet scales  $s = 5$ ,  $s = 3$ , and  $s = 1$ , both in the absence of chirp modulation ( $w_d = 0$ ) and for a chirp modulation with  $w_d = 1$ . Notice that these values have to be compared with the lower bound  $\mu(\text{F}, \Delta) = 3.906 \times 10^{-3}$ .

with the maximum complex modulus of the  $\mathbf{k}$ -space coefficient values of the modified sparsity basis vectors, which depend on the chirp modulation.

After normalization of the vectors of the sparsity and sensing bases in  $\ell_2$  norm, a simple numerical computation gives the mutual coherence between the sensing and sparsity bases for each desired value of the chirp rate  $w$ . Analyzing the impact of the chirp on the coherence between the sensing basis and the sparsity basis  $\Psi^{(s)}$  identifying each wavelet scale with  $1 \leq s \leq 5$  is very enlightening. The values of these coherences  $\mu(\text{FC}^{(w)}, \Psi^{(s)})$  are reported in Table 1. By definition, the overall coherence  $\mu(\text{FC}^{(w)}, \Psi)$  is the maximum over the values obtained at each wavelet scale. This maximum is naturally obtained for the lowpass filter ( $s = 5$ ), which is characterized by a smaller support in  $\mathbf{k}$ -space relative to the wavelets at scales  $s = 1$  to  $s = 4$ . Corresponding values for the overall coherence are reported in bold in Table 1.

Firstly, the overall coherence is smaller for  $w_d = 1$  than for  $w_d = 0$ , due to the spread spectrum phenomenon. In the context of compressed sensing, this result suggests that the quality of the  $\text{BP}_\epsilon$  reconstruction will be enhanced by the chirp modulation. Secondly, in the absence of chirp ( $w_d = 0$ ), the mutual coherence decreases toward its lower bound associated with the Dirac sparsity basis when the scale index  $s$  decreases. This natural behaviour simply illustrates the fact that waveforms with a smaller extent in image space are more spread in  $\mathbf{k}$ -space. This result suggests that, in the absence of chirp, the part of a signal associated with large wavelet scales will have a poor quality of the  $\text{BP}_\epsilon$  reconstruction relative to those associated with small wavelet scales. Thirdly, the coherence is affected very differently at each wavelet scale. For the smallest scales, the waveforms are already initially widely spread in  $\mathbf{k}$ -space so that the effect of the chirp is small, and actually null at four significant figures at  $s = 1$ . On the contrary, the effect gets more important when one considers larger wavelet scales  $s$ , indicating the effectiveness of the chirp in spreading the spectrum of the corresponding wavelets. This result suggests that the expected overall increase in the quality of the  $\text{BP}_\epsilon$  reconstruction should essentially be related to a better reconstruction of the part of the signal associated with large waveforms.

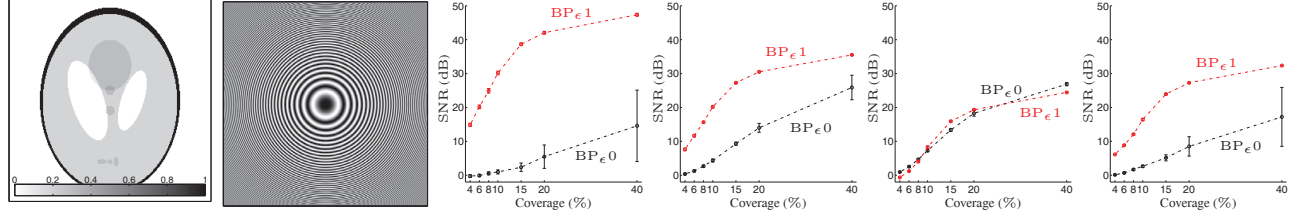


**Fig. 1.** First panel from the left: Shepp-Logan phantom on a grid of  $N$  pixels. Second panel from the left: real part of the chirp modulation with  $w_d = 1$ . The chirp is sampled on a grid of  $4N$  pixels in order to avoid any aliasing artifact. In both panels dark and light regions respectively correspond to positive and negative values. Other panels: SNR of reconstructions as a function of the coverage in  $k$ -space. The third, fourth and fifth panels from the left represent the SNR at the wavelet scales  $s = 5$ ,  $s = 3$ , and  $s = 1$  respectively, and the sixth panel from the left represents the SNR of the overall reconstruction. All SNR curves represent the mean SNR over 30 simulations, and the vertical lines identify the error at 1 standard deviation.

## 6. RESULTS

The results of the analysis are reported in Fig. 1. The reconstructions in the absence ( $w_d = 0$ ) and in the presence ( $w_d = 1$ ) of the chirp modulation are respectively denoted by  $BP_{\epsilon 0}$  and  $BP_{\epsilon 1}$ .

Firstly, as expected, for each coverage considered, the SNR for the overall reconstruction is significantly larger for  $BP_{\epsilon 1}$  than for  $BP_{\epsilon 0}$ . This is the spread spectrum phenomenon related to the reduction of the mutual coherence between the sensing basis and the sparsity basis in the presence of the chirp modulation. Secondly, for each coverage considered, the increase in the SNR of reconstruction is more important at large wavelet scales  $s$ , in complete agreement with our previous discussion. No significant increase is observed at  $s = 1$ , but well at larger scales. Finally, the enhancement can equivalently be cast in terms of a significant acceleration of the acquisition process for fixed reconstruction quality. Under the conditions of our simulations, a factor 4 or 5 can be inferred from the graph of the overall reconstruction SNR in Fig. 1.

## 7. CONCLUSION

We have considered probing MRI signals through an incomplete Fourier coverage, in the perspective of accelerating the acquisition process relative to a standard setting providing a complete coverage. In the context of compressed sensing, we have shown that pre-modulating signals by quadratic phase profiles would induce a spread spectrum phenomenon that could drastically enhance the quality of image reconstruction for sparse or compressible signals. Before stronger conclusions can be drawn, this approach should be extensively tested through real acquisitions, i.e. under real noise and coverage conditions in  $k$ -space.

## 8. REFERENCES

- [1] E.J. Candès, “Compressive sampling,” in *Proc. Int. Congress Math. Euro. Math. Soc.*, 2006, vol. 3., pp. 1433-1452.
- [2] J.G. Pipe, “Spatial encoding and reconstruction in MRI with quadratic phase profiles,” *Magn. Reson. Med.*, vol. 33, pp. 24-33, 1995.
- [3] S. Ito and Y. Yamada, “Alias-Free Image Reconstruction Using Fresnel Transform in the Phase-Scrambling Fourier Imaging Technique,” *Magn. Reson. Med.*, vol. 60, pp. 422-430, 2008.
- [4] A.A. Maudsley, “Dynamic range improvement in NMR imaging using phase scrambling,” *J. Magn. Reson.*, vol. 76, pp. 287-305, 1988.
- [5] V.J. Wedeen, Y.S. Chao, and J.L. Ackerman, “Dynamic range compression in MRI by means of nonlinear gradient pulse,” *Magn. Reson. Med.*, vol. 6, pp. 287-295, 1988.
- [6] M. Lustig, D. Donoho, and J. M. Pauly, “Sparse MRI: The Application of Compressed Sensing for Rapid MR Imaging,” *Magn. Reson. Med.*, vol. 58, pp. 1182-1195, 2007.
- [7] J. Haldar, D. Hernando, and Z.-P. Liang, “Compressed sensing in MRI with non-Fourier encoding,” 2008, (preprint <http://www.dsp.ece.rice.edu/cs>).
- [8] Y. Wiaux, G. Puy, Y. Boursier, and P. Vandergheynst, “Spread spectrum for imaging techniques in radio interferometry,” *Mon. Not. R. Astron. Soc.*, vol. 400, pp. 1029-1038, 2009.
- [9] G. Puy, Y. Wiaux, R. Gruetter, J.-Ph. Thiran, D. Van de Ville, and P. Vandergheynst, “Spread spectrum for interferometric and magnetic resonance imaging,” in *Proc. IEEE Int. Conf. on Acoustic, Speech and Signal Process.*, IEEE Signal Process. Soc., 2009, accepted for publication.